Contribution from the Department of Chemistry,
University of California, Davis, California 95616

Proton and Deuterium Nuclear Magnetic Resonance Studies on Iron(II) Complexes of N-Substituted Porphyrins

ALAN L. BALCH,* YEE-WAI CHAN, GERD N. LA MAR,* LECHOSLAW LATOS-GRAZYNSKI, and MARK W. RENNER

Received November 13, 1984

The proton NMR spectra of iron(II) monohalide complexes of *N*-methyltetraphenylporphyrin and *N*-methyloctaethylporphyrin have been recorded and assigned by means of specific deuteration, methyl substitution, intensity, and line width considerations. The *N*-methyl resonance appears at a characteristic position at 68–145 ppm and is particularly readily observed by ^{2}H NMR spectroscopy on deuterium-labeled samples. The ^{1}H NMR spectra of the iron(II) porphyrin complex bearing an *N*-CH=C(*p*-$C_6H_4Cl)_2$ substituent and the iron(III) porphyrin complex with a C=C(*p*-$C_6H_4Cl)_2$ unit inserted into one Fe—N bond are distinct although both spectra are consistent with C_s symmetry for their respective complexes. Imidazole replaces the axial halide ligand to produce derivatives that give clearly resolved resonances of the coordinated amine at −50 °C. Both the *N*-methyl and the histidine *N*-H resonances should be readily detected and assigned in proteins containing iron(II) *N*-methylporphyrin.

Introduction

The biological significance of N-substituted porphyrins, **1**, has only recently been recognized. Inactivation of hepatic cytochrome

1

P-450 by a variety of substances, including, as the simplest, ethylene, leads to the formation of abnormal green pigments that have been shown to be N-substituted porphyrins.[1-3] Likewise oxyheme proteins react with phenylhydrazine to form *N*-phenylprotoporphyrin IX.[4,5] It is likely that iron complexes of these N-substituted porphyrins are involved as intermediates in these transformations. Particularly relevant in this regard is the recent demonstration of transfer of an alkyl or aryl group from iron to nitrogen in porphyrin complexes.[6,7]

Proton NMR spectroscopy has been shown to be a uniquely definitive method for detecting and characterizing iron porphyrins.[8] The hyperfine shift patterns that have been recorded for paramagnetic iron porphyrins are sensitive to the iron oxidation, spin, and ligation states. Proton NMR spectroscopy should also be effective in characterizing metal complexes of N-substituted porphyrins. For materials derived from synthetic porphyrins with symmetrical peripheral substitution, the spectra are expected to be inherently more complex because of the reduction in symmetry from D_{4h} to C_s that occurs upon N-substitution.

Here we report on the ^{1}H and ^{2}H NMR spectra of the iron(II) complexes **2–8** and their zinc(II) analogues **9** and **10**.[9-11] The high spin ($S = 2$) *N*-alkyl iron(II) complexes, unlike their non-alkylated counterparts, are air stable.[9] The geometric details of the structure of **2** are known from an X-ray single-crystal

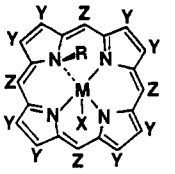

2-10

	M	R	Y	Z	X
2	Fe	CH_3	H	C_6H_5	Cl
3	Fe	CH_3	H	C_6H_5	Br
4	Fe	CH_3	H	C_6H_5	I
5	Fe	CH_3	H	*p*-$C_6H_4CH_3$	Cl
6	Fe	CH=C(*p*-$C_6H_4Cl)_2$	H	C_6H_5	Cl
7	Fe	CH_3	CH_2CH_3	H	Cl
8	Fe	CH_3	CH_2CH_3	H	Br
9	Zn	CH_3	H	C_6H_5	Cl
10	Zn	CH=C(*p*-$C_6H_4Cl)_2$	H	C_6H_5	Cl

diffraction study.[9] The present work has been designed to identify characteristic resonance patterns for synthetic porphyrins and chemical shift information relevant to natural porphyrins so that the identification of these complexes is facilitated. Additionally the binding of an external base, imidazole, to these complexes has been examined. Imidazole serves here as a model for histidine, which frequently is found as a ligand in heme proteins. Although the binding of a thiol would have been more relevant toward providing models for cytochrome P-450, the known sensitivity of these iron(II) complexes toward thiols[10] limited us to examining imidazoles. Finally these N-substituted complexes are compared to their iron(III) carbene counterparts, **11**.[12-15] For symmetrical

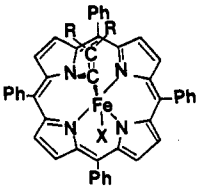

11, R = *p*-C_6H_4Cl

synthetic porphyrins, both the N-substituted complexes and the carbene complexes have C_s symmetry. The two complexes **6** and **11** differ by only one electron and one proton. Consequently it is important to establish characteristic spectroscopy differences between these closely related types of complexes. Brief descriptions of this[16] and somewhat related observations[17] have been presented.

(1) Ortiz de Montellano, P. R.; Beilan, H. S.; Kunze, K. L.; Mico, B. A. *J. Biol. Chem.* **1981**, *256*, 4395.
(2) Ortiz de Montellano, P. R.; Beilan, H. S.; Kunze, K. L. *J. Biol. Chem.* **1981**, *256*, 6708.
(3) Ortiz de Montellano, P. R.; Kunze, K. L.; Beilan, H. S.; Wheeler, C. *Biochemistry* **1982**, *21*, 1331.
(4) Saito, S.; Itano, H. A. *Proc. Natl. Acad. Sci. U.S.A.* **1981**, *78*, 5508.
(5) Augusto, O.; Kunze, K. L.; Ortiz de Montellano, P. R. *J. Biol. Chem.* **1982**, *257*, 6231.
(6) Ortiz de Montellano, P. R.; Kunze, K. L.; Augusto, O. *J. Am. Chem. Soc.* **1982**, *104*, 3545.
(7) Mansuy, D.; Battioni, J.-P.; Dupre, D.; Satori, E.; Chottard, G. *J. Am. Chem. Soc.* **1982**, *104*, 6159.
(8) La Mar, G. N.; Walker (Jensen), F. A. In "The Porphyrins"; Dolphin, D., Ed.; Academic Press: New York, 1979; Vol. 4, p 61.
(9) Anderson, O. P.; Kopelove, A. B.; Lavallee, D. K. *Inorg. Chem.* **1980**, *19*, 2101.
(10) Lavallee, D. K. *J. Inorg. Biochem.* **1982**, *16*, 135.
(11) Lavellee, D. K.; Kopelove, A. B.; Anderson, O. P. *J. Am. Chem. Soc.* **1978**, *100*, 3025.
(12) Chevrier, B.; Weiss, R.; Lange, M.; Chottard, J.-C.; Mansuy, D. *J. Am. Chem. Soc.* **1981**, *103*, 2899.
(13) Latos-Grazynski, L.; Cheng, R. J.; La Mar, G. N.; Balch, A. L. *J. Am. Chem. Soc.* **1981**, *103*, 4270.
(14) Olmstead, M. M.; Cheng, R.-J.; Balch, A. L. *Inorg. Chem.* **1982**, *21*, 4143.

0020-1669/85/1324-1437$01.50/0

Table I. ^{1}H NMR Data for Iron(II) and Zinc(II) N-Substituted Tetraarylporphyrin Complexes

	chem shift, ppm (line width, Hz)						
	2[a]	3[b]	4[b]	5[a]	6	9	10
pyrrole	41.9 (97)	46.4 (81)	54.7 (56)	42.0	48.8 (124)	8.30	7.90
	31.7 (62)	32.3 (32)	33.9 (38)	31.1	27.4 (43)	8.97[f]	8.82[g]
	−0.25 (137)	3.0 (89)		0.26	7.9 (145)	8.84[f]	8.75[g]
	−0.44 (79)	0.1 (52)		0.12	0.9 (78)	8.92	8.93
ortho phenyl	14.6 (60)	15.2	16.4	14.6	20.1 (72)	8.62 (2 H)[j]	8.30 (2 H)
	6.5 (89)	8.3	9.4	6.2	3.1 (93)	8.13 (2 H)[j]	8.13 (2 H)[k]
	5.1 (82)	7.4	8.8	5.0	0.0 (67)	8.32 (4 H)	8.07 (2 H)[k]
	4.3 (51)	5.9		4.4	−0.5 (44)		
meta phenyl	9.4			9.2	10.7	7.93–7.76 (12 H)	7.85–7.72 (14 H)
	9.3			9.1	9.5		
	8.5			8.2	7.5		
	6.8			6.6	5.3		
para phenyl	8.3			4.4	8.4		
	6.6			3.0	5.6		
R–N	105 (973)	92 (733)	68 (484)	104	161 (125)[d,e]	−3.83	−2.24[d]
					14.6 (45)		7.37[h]
					11.8 (530)		5.77[h]
					4.7 (12)		5.75[i]
					−7.8 (48)		2.99[i]

[a] 23 °C, $CDCl_3$ (line width at 0 °C). [b] 23 °C, $CDCl_3$. [c] 21 °C, $CDCl_3$ (line width at −5 °C). [d] Vinyl CH. [e] From ^{2}H NMR. [f] Coupled; J = 4.6 Hz. [g] Coupled; J = 4.8 Hz. [h] Coupled; J = 8.3 Hz. [i] Coupled; J = 7.4 Hz. [k] Coupled; J = 7.0 Hz.

Results

Characteristics and Spectral Assignments for Halide Complexes. The NMR data have been analyzed in the context of the C_s geometry shown in **12**. In this case there are four distinct pyrrole

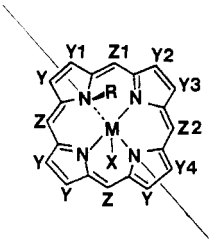

12

positions, Y1–Y4, and two meso positions, Z1 and Z2. With phenyl rings in both of the two meso positions, it may be anticipated that the ortho and meta positions on each ring will be distinguishable due to the essentially perpendicular relationship between the phenyl plane and the plane of the adjacent pyrrole ring and the restricted rotation about the meso-carbon-to-phenyl bond. For ethyl groups bound to the pyrrole sites, Y1–Y4, the methylene groups will be diastereotopic. Thus eight methylene hydrogen environments will be present while only four methyl environments are anticipated.

The ^{1}H NMR spectrum of the N-methyl complex **2** is shown at the bottom (trace A and A′) of Figure 1. This spectrum was recorded at −50 °C, where all individual resonances are clearly resolved. Resonance assignments, which are given above each peak, have been made on the basis of relative intensities, line widths, site-specific deuteration, and methyl substitution. The most characteristic feature, the downfield peak at 142 ppm, has been identified as the N-methyl resonance. The ^{2}H NMR spectrum of **1** with R = CD_3 is shown in inset B′ of Figure 1. The spectrum contains only the N-CD_3 resonance at 138 ppm. The magnitude and direction of the isotope effect on the chemical shift of this group are entirely consistent with previous observations

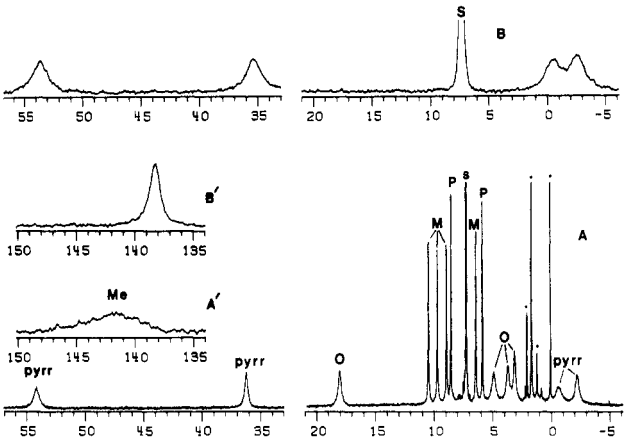

Figure 1. NMR spectra of the N-methyl iron(II) complex **2** in chloroform-d_1 solution at −50 °C. Traces A and A′ are the 360-MHz ^{1}H spectra. Trace B shows the 76.7-MHz ^{2}H NMR spectrum of deuterated-pyrrole **2** (Y = D) while trace B′ shows the ^{2}H spectrum of deuterated-methyl **2** (R = CD_3). Resonance assignments: Me, N-methyl; pyrr, pyrrole; o, m, or p, ortho, meta, or para phenyl; S, solvent; *, impurities.

on ^{1}H and ^{2}H NMR spectra of paramagnetic molecules.[18] The ^{2}H NMR spectrum of deuterated-pyrrole **2** (Y = D) is shown in trace B of Figure 1. In accord with the C_s structure, there are four pyrrole resonances. The ten additional resonances in trace A of Figure 1 come from the phenyl protons. The two para proton resonances have been unambiguously identified since these resonances are missing in the spectrum of the p-tolyl derivative **5** and two new methyl resonances are present. The remaining eight resonances fall into two groups according to their line widths. The four broad lines are assigned to the ortho phenyl protons since these will be relaxed more efficiently because they are closer to the paramagnetic iron ion. The four narrow resonances are assigned to the meta phenyl resonances.

A Curie plot for the N-methyl and the pyrrole resonances of **2** is given in Figure 2. While the experimental data show linear behavior, the extrapolated intercepts are fairly far from the diamagnetic positions, which may be estimated from the data for the zinc complex **9**.

The ^{1}H NMR data for the complexes studied here are set out in Table I. Spectral assignments for the N-methyl complexes

(15) Mansuy, D.; Morgenstern-Badarau, I.; Lang, M.; Gans, P. *Inorg. Chem.* **1982**, *21*, 1427.
(16) Balch, A. L. "Abstracts of Papers", 185th National Meeting of the American Chemical Society, Seattle, WA, March 1983; American Chemical Society: Washington, DC, 1983; INOR 176.
(17) Goff, H. M.; Shirazi, A.; Boersma, A. D.; Godziela, G. M.; Coulthard-Lynn, J. C. "Abstracts of Papers", 185th National Meeting of the American Chemical Society, Seattle, WA, March 1983; American Chemical Society: Washington, DC, 1983; INOR 255.
(18) Horn, R. R.; Everett, G. W., Jr. *J. Am. Chem. Soc.* **1971**, *93*, 7173.

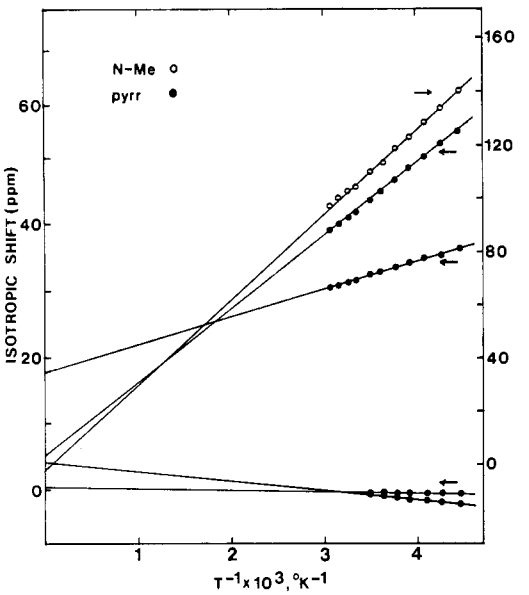

Figure 2. A Curie plot for the *N*-methyl and pyrrole protons of the *N*-methyl iron(II) complex **2** in chloroform solution.

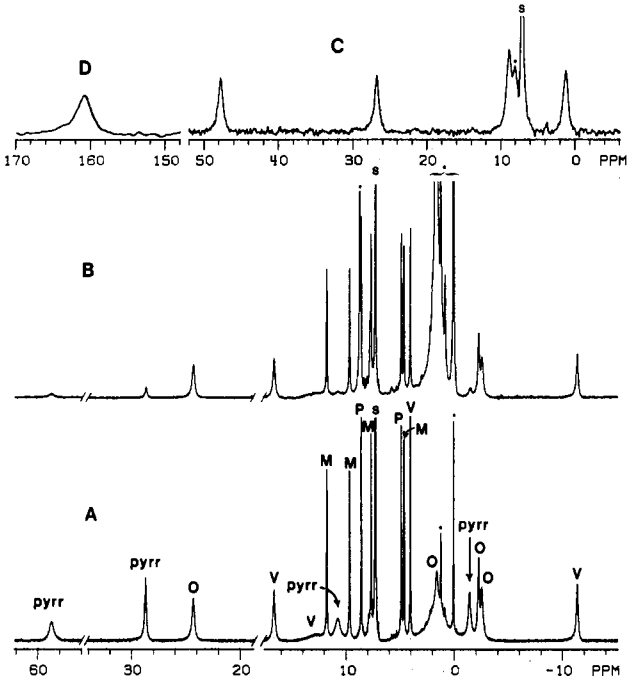

Figure 3. NMR spectra of the *N*-vinyl iron(II) complex **6** in chloroform-d_1 solution at −30 °C. Trace A shows the 360-MHz ^{1}H NMR spectrum at the unlabeled sample while trace B shows the same spectrum for the deuterated-pyrrole form **6** (Y = D). Trace C shows the 55-MHz ^{2}H NMR spectrum at 25 °C for deuterated-pyrrole **6** (Y = D). Trace D shows the 76.7-MHz ^{2}H NMR spectrum of CD-labeled-vinyl **6** (R = CD=C(p-$C_6H_4Cl)_2$) at 23 °C. Assignments follow those in Figure 1 except V, protons of the vinyl phenyl groups.

2–**5** follow from the information presented above. Changes in the axial anion X produce shifts in resonance positions up to 37 ppm, but they do not alter the pattern of the shifts. The effect of the axial anion on the *N*-methyl resonance is particularly pronounced.

The ^{1}H NMR spectrum of the *N*-vinyl complex **6** is shown in trace A of Figure 3. The four pyrrole resonances have been identified by deuterium labeling. Trace B of Figure 3 shows the ^{1}H NMR spectrum of deuterated-pyrrole **6** (Y = D). The four pyrrole peaks have diminished intensity. The ^{2}H NMR spectrum of this same sample at a different temperature is shown in trace C. The four equally intense pyrrole resonances are readily seen. The pattern of these pyrrole resonances is similar to that already

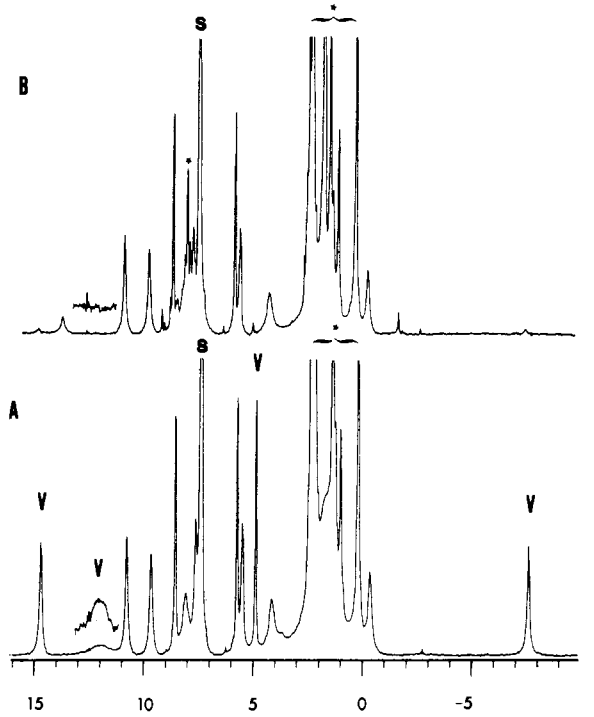

Figure 4. The 360-MHz ^{1}H NMR spectra of (A) the *N*-vinyl iron(II) complex **6** and (B) *N*-vinyl deuterated-phenyl **6** (R = CH=C(p-$C_6D_4Cl)_2$) in chloroform-*d* at 23 °C.

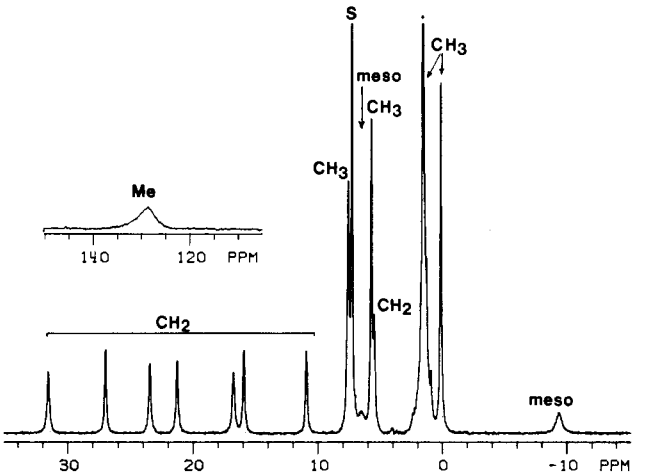

Figure 5. The 360-MHz ^{1}H NMR spectrum of the *N*-methyloctaethylporphyrin iron(II) complex **7** in chloroform-*d* at 10 °C.

seen for the *N*-methyl complex **2**. The resonance of the unique vinyl CH unit has been detected by ^{2}H NMR spectroscopy. The ^{2}H NMR spectrum of **6** (R = CD=C(p-$C_6H_4Cl)_2$) consists of the single broad (line width 125 Hz) resonance at 161 ppm, which is shown in inset D of Figure 3. This feature was not detected in the ^{1}H NMR spectrum of **6**, but this is not unexpected since the extrapolated line width for the corresponding ^{1}H resonance would be 5 Hz. This suggests that the vinyl CH is very close to the iron atom. Deuteration of the phenyl groups of the *N*-vinyl substituent allows for their assignment as shown in Figure 4. Trace A shows the relevant region for **6** while trace B shows the same region for **6**, R = CH=C(p-$C_6D_4Cl)_2$. In trace B four resonances, those of the ortho and meta protons of the two distinct phenyl groups of the *N*-vinyl substituent, have decreased in intensity. The ten phenyl resonances from the meso substituents have been assigned by the procedure described in the analysis of the spectrum of **2**.

Figure 5 shows the ^{1}H NMR spectrum of the *N*-methyloctaethylporphyrin complex **7**. The characteristic downfield resonance of the *N*-methyl group appears at 130 ppm. Eight equally intense resonances in the 35–5 ppm region are assigned to the methylene

Table II. ^{1}H NMR Data for Iron(II) Complexes of *N*-Methyloctaethylporphyrin

	7 (X = Cl)[a]	8 (X = Br)[a]
meso	6.7	10.5
	−8.7 (164)	−3.5 (128)
methylene	30.2	33.5
	26.0	26.6
	22.5	25.8
	20.5	23.3
	16.2	19.2
	15.4	16.7
	10.5	11.6
	5.4	5.9
methyl	7.3	10.0
	5.5	7.3
	2.05	1.8
	0.21	0.31
N-CH_3	121 (1290)	103 (922)

[a] 23 °C, $CDCl_3$ (line width, Hz).

protons on the basis of their relative areas and their similar line widths. Four methyl resonances are present, as are two meso proton resonances at 6.5 and −9.8 ppm. Data for this complex and its bromo analogue **8** are presented in Table II.

Imidazole Coordination. The addition of imidazole and methylimidazoles has been followed by ^{1}H NMR spectroscopy. Titration of a 2 mM solution of the *N*-methyl complex **2** with imidazole in chloroform-*d* at −50 °C produces the gradual growh of a new set of resonances while the resonances of **2** diminish in intensity. The spectrum of the product is shown in trace A of Figure 6. Resonances of the coordinated imidazole are clearly discernible. Their integrated intensity relative to the pyrrole and phenyl resonances indicates that only one imidazole ligand is bound. An identical spectrum is obtained when the bromo complex **3** is used in place of the chloro complex **2**. This observation along with the fact that the overall pattern of the porphyrin resonance positions and relative line widths appears to be retained in the spectrum of the imidazole adduct indicates that imidazoles has replaced the axial anion in **2** and **3** to form the salt **13**. The identity of the two downfield pyrrole resonances has been established by deuteration of the pyrrole sites and noting the absence of these resonances in the appropriate spectrum.

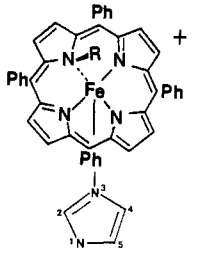

13, R = CH_3

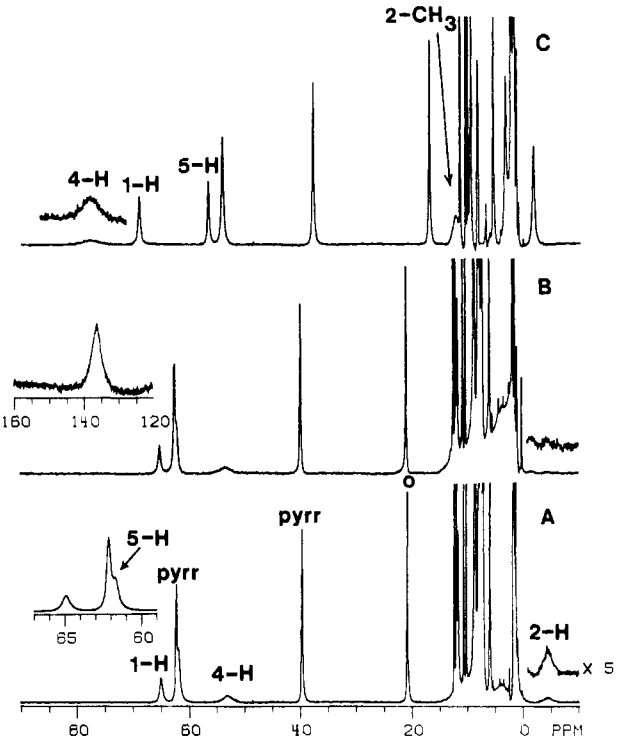

Figure 6. The 360-MHz ^{1}H NMR spectra of a 2 mM chloroform-*d* solution of the *N*-methyl complex **2** in the presence of 40 mM (A) imidazole, (B) imidazole-*2-d*, and (C) 2-methylimidazole. The insert in trace B shows the *N*-methyl resonance. Analogous features are present in the spectra corresponding to traces A and C but are not shown.

From the titration data the binding constant for the formation of **13** from 1-methylimidazole in chloroform-*d* at −50 °C has been found to be 1 M^{-1}. Titrations of mixtures of the chloro and bromo complexes **2** and **3** show that the bromo complex **3** reacts preferentially with imidazole, a result that is in accord with the preference of the hard iron center for the harder of the two halide ligands. The stronger base, imidazole, binds to **2** with a binding constant that is about an order of magnitude greater than that for 1-methylimidazole.

The imidazole resonances have been identified through suitable substitution. The data are summarized in Table III. The spectrum obtained from imidazole-*2-d* is shown in trace B of Figure 6. The resonance of the 2-H is readily assigned since it is missing in trace B. The resonance of the 4-H is assigned on the basis of its line width, which is similar to that of the 2-H resonance. Both are expected to be at similar distances from the iron, and both should have comparable widths that are greater than those of the other imidazole resonances. The 1-H resonance has been assigned to the peak at 63.1 ppm since that peak is absent from the spectrum obtained from 1-methylimidazole. The

Table III. NMR Data for the Imidazole Complexes, 13

	imidazole[a]			1-methylimidazole[a]			2-methylimidazole[a]		
position	chem shift, ppm	line width, Hz	isotropic shift,[b] ppm	chem shift, ppm	line width, Hz	isotropic shift,[b] ppm	chem shift, ppm	line width, Hz	isotropic shift,[b] ppm
N-H	64.9	230	52.2				68.9	154	52.3
2-H	−4.5	700	−4.5	−5.0	560	−6.0			
4-H	53.2	730	52.7	62.2	590	61.8	77.7	1015	52.6
5-H	61.7	150	57.3	63.1	170	58.7	56.4	121	57.5
1-CH_3				23.8	112	22.1			
2-CH_3							12.1	590	14.6
N-CH_3	135	1030		136	890		155	1230	
pyrrole	62	120		65	91		53.9	143	
pyrrole	39.5	68		39	66		37.7	93	
ortho phenyl	20.7	53		20.8	52		16.9	72	

[a] In $CDCl_3$ at −50 °C. [b] Reference is the diamagnetic ruthenium(II) complex: Satterlee, J. D.; La Mar, G. N. *J. Am. Chem. Soc.* 1976, *98*, 2804.

spectrum of the 2-methylimidazole complex is shown in trace C of Figure 6. The 2-CH_3 resonance is readily assigned. There is a significant shift in the pattern of the other imidazole resonances, with the broadest resonance, the one assigned to the 4-H, being shifted to lowest field. These changes are no doubt a consequence of the steric effects resulting from the introduction of the methyl group so close to the metal binding site of the imidazole.

The binding constant for imidazole coordination is strongly temperature dependent. Warming a sample of **13** (X = Cl) results in the gradual decrease in intensity of the characteristic porphyrin resonances of **13** and the growth in intensity of the corresponding resonances of the parent **2**. This behavior is fully reversible with temperature. At room temperature the binding constant is so small that, for reasonable concentrations of imidazole and the iron complex, no adduct formation is detected.

Discussion

Neutral Halide Complexes. The NMR results for these synthetic porphyrins are fully in accord with the C_s structure **12**. For the *N*-methylporphyrins, the most characteristic feature of their iron(II) complexes is the extreme downfield shift for the *N*-methyl group. Such large downfield shifts are common for *N*-alkyl groups in a variety of paramagnetic complexes; they generally reflect a downfield σ-spin transfer mechanism.[19,20] Since this feature is sharp and easily detected in the ^2H NMR spectrum of the deuterated derivative, it appears that ^2H NMR spectroscopy on suitably deuterated samples would be the technique of choice to use to identify other substituents that might become attached to the porphyrin nitrogens through heme degradation. As an example, the unique vinyl proton of **6** could only be detected in the ^2H NMR spectrum. Other characteristic porphyrin resonances that are shifted out of the normal diamagnetic region include the two pyrrole protons that occur in the 25–60 ppm region, the pyrrole methylene protons (and by inference pyrrole methyl protons), which appear in the region 35–5 ppm, and the meso proton, which occurs upfield at −9.5 ppm. Of course for synthetic porphyrins with symmetrical peripheral substitution, the overall reduction in symmetry and increase in spectral complexity are prominent spectral characteristics. The hyperfine shift pattern for the same peripheral substituents has some resemblance to other normal high-spin iron(II) complexes.[21] Two of the pyrrole peaks in **2**, **3**, and **4** resonate at essentially the same position as the single peak in fourfold symmetric derivatives.

The NMR spectrum of the N-substituted porphyrin complex **6** is clearly different from that of the carbene insertion product **11**, an iron(III) complex. Both spectra reflect the idealized C_s symmetry of the two complexes, but the hyperfine shift patterns are readily distinguishable. The ^1H NMR spectrum of **11** (X = I) has been reproduced in ref 13. In it three of the pyrrole resonances are shifted well upfield (δ −42.3, −29.3, −21.2 for X = I;[13] δ −40.5, −23.9, −19.7 for X = Cl[22]) while one is shifted downfield (δ 21.6 for X = I; δ 25.7 for X = Cl[22]). The resonance of the phenyl protons of vinylcarbene in **11** appear in an upfield region (δ −7.4, −0.2, 1.8, 3.2 for X = I; δ −0.2, 2.7, 3.6 for X = Cl with the broad upfield resonance not observed[22]). In contrast in **6**, two of the vinyl phenyl resonances occur in a downfield shifted region at 14.5 and 12 ppm. Finally the unique vinyl CH resonance in **6** has been detected. It occurs in the downfield region that one would expect from the results for the *N*-methyl analogues. Naturally, this has no counterpart in the spectrum of **11**.

Magnetic Properties. Information on the nature of iron–porphyrin bonding is contained in the contact shift, $(\Delta H/H)^{con}$, which, together with the dipolar shift, $(\Delta H/H)^{dip}$, make up the observed hyperfine shift, $(\Delta H/H)^{hf}$, i.e.

$$(\Delta H/H)^{hf} = (\Delta H/H)^{con} + (\Delta H/H)^{dip}$$

The dipolar contribution is given by

$$(\Delta H/H)^{dip} = \Delta\chi_1(3\cos^2\theta - 1)r^{-3} + \Delta\chi_2(\sin^2\theta\cos 2\Omega)r^{-3}$$

where $\Delta\chi_1 = {}^1/_3[\chi_{zz} - {}^1/_2(\chi_{xx} + \chi_{yy})]$, $\Delta\chi_2 = {}^1/_2(\chi_{xx} - \chi_{yy})$, χ_{ii} are the principal components of the susceptibility tensor (z parallel to original fourfold axis and x passing through N-CH_3 and iron), θ is the angle of the iron–proton vector to the z axis, Ω is the angle of the projection of the vector onto the xy plane and the x axis, and r is the length of this vector. If we make the simplifying but realistic assumption that, with an axial halide, the system will still exhibit primarily an axial distortion with only a subsidiary rhombic distortion, it can be shown that both axial and rhombic anisotropies (and hence dipolar shifts) are negligible.

Thus the essentially perpendicular orientation of the four meso-phenyl groups with respect to the porphyrin plane dictate that the rhombic dipolar shift is zero because for $\Omega = 45°$, the second term is zero independent of $\Delta\chi_2$. Moreover, if axial anisotropy is significant, the relative geometric factors for the three phenyl substituents demand dipolar shifts in the same direction and of relative magnitude *o*-H > *m*-H > *p*-H. Although a single *o*-H and one *m*-H show shifts larger than the others, one set of phenyl groups must exhibit upfield *o*-H, *p*-H and downfield *m*-H shifts of essentially the same magnitude. The pattern is consistent with π-spin delocalization and argues strongly for a negligible axial anisotropy for one ring, and thus for the whole complex. In the absence of significant axial anisotropy, we conclude that the in-plane anisotropy must also be negligible. These conclusions are consistent with the small anisotropy characterized for high-spin iron(II) complexes for a variety of axial ligands.[21–23]

Electronic Structure. The observed pyrrole hyperfine shifts, which thus are predominantly contact, must reflect the lowering of the symmetry on the bonding. While it is logical to assign one of the pyrrole-H peaks with small contact shift to the unique N-methylated pyrrole, we have no information as to how to assign the other three. If the second pyrrole H with small shift is assigned to the trans pyrrole, arguments could be invoked concerning the raising of the d_{xz}, d_{yz} (e_π^*) orbital degeneracy, as found to be applicable to distorted low-spin iron(III) system.[24–26] However, precedence[27] exists also for neighboring protons on the same pyrrole to exhibit widely different magnitudes of spin density. Consequently, in the absence of individual assignments, any detailed interpretation of the bonding would be too speculative.

It has already been concluded that the somewhat small shifts and odd pattern for the contact shifts in high-spin iron(II) complexes arise from near cancellation of effects of unpaired spin density of opposite signs resulting from spin delocalization in σ as well as both filled $3e(\pi)$ and vacant $4e(\pi^*)$ molecular orbitals.[8,19,24–26] The lower symmetry in the present case must result in variable changes in each of the interactions with each of the pyrroles and may not lend itself to interpretation at this time without individual assignments and/or additional ^{13}C data.

The R resonances in **6** could not be assigned to individual phenyl groups. However, the broadest signal at 12 ppm must come from the *o*-H of the ring over the iron. In fact, the nonorthogonality of the σ and π systems at the pyrrole nitrogen would lead to expected π-spin delocalization into the two *p*-chlorophenyl substituents such that both rings exhibit downfield *o*-H and upfield *m*-H contact shifts, consistent with a pair of upfield and downfield peaks for the substituent.[28]

Line Width Results. Two line width effects are apparent in the present complex. In the isostructural series **2**, **3**, **4**, where the axial halide is varied, all line widths vary in the order Cl > Br > I, as found previously for both high-spin and intermediate-spin iron(III) complexes.[29] The proton line widths, δ, in these complexes are

(19) Fitzgerald, R. J.; Drago, R. S. *J. Am. Chem. Soc.* **1968**, *90*, 2523.
(20) Del Gaudio, J.; La Mar, G. N. *J. Am. Chem. Soc.* **1978**, *100*, 1112.
(21) Goff, H.; La Mar, G. N. *J. Am. Chem. Soc.* **1977**, *99*, 6599.
(22) Balch, A. L.; Cheng, R.-J.; La Mar, G. N.; Latos-Grazynski, L., to be submitted for publication.
(23) Parmely, R. C.; Goff, H. M. *J. Inorg. Biochem.* **1980**, *12*, 269.
(24) Traylor, T. G.; Berzinis, A. P. *J. Am. Chem. Soc.* **1980**, *102*, 2844.
(25) Goff, H. *J. Am. Chem. Soc.* **1980**, *102*, 3252.
(26) Walker, F. A.; Buehler, J.; West, J. T.; Hinds, J. L. *J. Am. Chem. Soc.* **1983**, *105*, 6923.
(27) Mispelter, J.; Momenteau, M.; Lhoste, J.-M. *Biochimie* **1981**, *63*, 911.
(28) Eaton, D. R. In "NMR of Paramagnetic Molecules"; La Mar, G. N., Horrocks, W. D., Jr., Holm, R. H., Eds.; Academic Press: New York, 1973; p 179.
(29) La Mar, G. N.; Walker, F. A. *J. Am. Chem. Soc.* **1973**, *95*, 6950.

dominated by proton–electron dipolar relaxation for which the correlation time is the electron spin relaxation time, T_{1e}, so that $\delta \propto T_{1e}$. T_{1e}, in turn, is determined by modulation of the zero-field splitting constant, D, so that $T_{1e} \propto D^{-2}$. This leads to a qualitative relation between line width and the magnitude of the zero-field splitting constant, $\delta \propto D^{-2}$. Thus we conclude that D (for assumed dominant axial distortion) increases in the order Cl < Br < I, as was found to be the case for iron(III) complexes.[29] Since the axial field is weakest for I, it can be concluded that D is negative for the present complexes.[29]

The second observed line width phenomenon involves the variable line width exhibited by the four pyrrole-H signals. While the alkylated pyrrole does have its protons closer (4.9 Å) than the other three pyrroles (5.1 Å),[9] the difference in pyrrole-H line widths exceeds that predicted by dipolar relaxation and cannot account for the indicated difference for the three more "normal" pyrroles. Since the line widths also fail to correlate with the magnitude of the contact shift, as might be expected from scalar relaxation, we suggest that one origin could be either from large delocalized spin density at position adjacent to the proton-bearing carbons[30] or from additive relaxation effects from delocalized spin density, which may yield small contact shifts due to the difference in sign of the coupling constant (A) (relaxation depends on a A^2 and hence $|A|$).[31] Individual pyrrole-H assignments and ^{13}C data again could shed further light on the highly interesting shift and relaxation patterns in these novel complexes.

Imidazole Adducts. The small difference in shifts for the two resolved pyrrole H's in the halide and imidazole adducts indicates that the metal–porphyrin interactions are essentially the same. While the pyrrole-H shifts are insensitive to the imidazole substituent, the N-CH_3 shift is larger for 2-methylimidazole than for imidazole or 1-methylimidazole, probably due to the increased basicity of the former ligand. In this sense, the stronger axial base causes a downfield bias for the N-CH_3 whether the halide or imidazole substituent is varied. The strong similarity in both the pyrrole-H and phenyl hyperfine shift patterns in the halide and imidazole complex allows us to conclude that the shift origins are predominantly contact also for the latter complexes. In this case, the hyperfine shift pattern for the axial base is also predominantly contact.

The shifts for the various imidazole protons, as listed in Table III, are downfield for all positions except 2-H and downfield for both proton and methyl groups at position 1. This pattern is generally consistent with major contributions from σ-spin delocalization,[32] although a sign change at the 2-position suggests nonnegligible contribution from π bonding. The lowest unoccupied π MO of imidazole exhibits by far the largest spin density at the 2-C[33] so that some contribution from Fe → Im π charge transfer is consistent with the small upfield 2-H shift.

Comparison in Table III of the present imidazole contact shifts with those reported earlier[21] for normal high-spin iron(II) porphyrin complexes reveals similarities in the patterns but substantial differences in the magnitudes. Except for the 2-position where the two spin-delocalization mechanisms are comparable and tend to cancel, the shift patterns are close. The cause of the smaller shifts (by nearly a factor of 2 is some cases) for the N-methylporphyrins is not understood. The crystal structure of **2** does not indicate any obvious steric constraints that would allow ready rationalization of the apparent reduction in axial covalency in N-methyl relative to normal ferrous porphyrins.

Thus we conclude that adducts of iron(II) N-methylporphyrins exhibit highly characteristic N-CH_3 hyperfine shifts in the low-field window, 100–150 ppm, irrespective of the exact nature of the axial ligand and that the N-methylation also induces a significant reduction in the σ covalency of axial imidazoles.

Relevance to Protein Structure. The hyperfine shift patterns for the model complexes of ferrous N-methylporphyrins present several useful and potentially unique probes for detecting this species in hemoproteins by ^1H NMR spectroscopy. Not only does the characteristic large downfield N-methyl (or N-aryl) contact shift provide a clear signal in a unique window (100–150 ppm) for a range of axial ligands for nonlabile protons in any reduced iron protein for which the ^1H NMR spectrum has been reported but the potential for effecting the N-alkylation using deuterated reagents also provides an unambiguous method for verifying the signal assignments. Moreover, if the substituent exhibits too broad a ^1H signal, ^2H NMR detection will be possible because of the significantly reduced (factor ~42) dipolar line width, and the internal rotation of a small substituent (methyl) will diminish quadrupolar line broadening by factor of ~9.[34] Thus in a protein of mol mass 16 000–64 000 daltons line widths of only 40 and 120 Hz can be anticipated for the N-CH_3 group. Such signals are readily detected by ^2H NMR in 1 mM solutions.

For the case of alkyl or aryl migration to a pyrrole nitrogen effected in myoglobin or other hemoprotein possessing axial histidyl imidazoles, the unique window for the sole labile coordinated imidazole ring NH signal downfield of the diamagnetic envelope should serve as an important seconding confirmation for N substituents. In normal high-spin reduced hemoproteins of various sorts (peroxidase,[35] myoglobin,[36] hemoglobin,[36] cytochromes c')[37] this signal is found in the region 60–85 ppm, with that in unstrained deoxymyoglobin and model compounds[36] essentially the same at 77 ppm. Our N-methylporphyrin models indicate that the shift is reduced by nearly a factor of 2, suggesting that the as yet unreported N-methyldeoxymyoglobin should exhibit the proximal histidyl imidazole ring NH signal in the region 35–40 ppm at room temperature.

Experimental Section

Chloroform-d_1 (Aldrich) was dried over molecular sieves. Tetrahydrofuran (THF) was distilled from sodium/benzophenone under a nitrogen atmosphere. 1-Methylimidazole (1-MeIm) (Aldrich) was distilled at reduced pressure and stored over molecular sieves. Octaethylporphyrin ($OEPH_2$) (Aldrich) was used without further purification. Tetraphenylporphyrin ($TPPH_2$), tetra-p-tolylporphyrin ($TpTPH_2$), and pyrrole-d_8 tetraphenylporphyrin were prepared and purified using literature procedures.[38,39] Imidazoles were purified by standard procedures.[33] Imidazole-*2-d* was prepared by a standard method.[40]

***N*-Alkylporphyrins.** N-CH_3TPPH, N-CH_3TpTPH, N-CH_3TPPH-*pyrr*-d_8, and N-CH_3OEPH were synthesized by reacting the appropriate porphyrin with either methyl iodide or dimethyl sulfate as the methylating agent.[41] N-CD_3TPPH was synthesized by using dimethyl-d_6 sulfate (Sigma). The reaction mixture was neutralized and then chromatographed on a basic alumina column. The unreacted starting material was eluted with a 10:1 v/v toluene–ethyl acetate solution. The N-methylporphyrin was eluted with chloroform and recrystallized from 1:1 v/v chloroform–methanol. The N-methylporphyrins were characterized by their distinct ^1H NMR and electronic absorption spectra.[41]

N-CH=C(p-C_6H_4Cl)$_2$TPPH, N-CH=C(p-C_6D_4Cl)$_2$TPPH, and N-CH=C(p-C_6H_4Cl)TPPH-*pyrr*-d_8 were synthesized by reacting a dichloromethane solution of the appropriate form of **11** (X = Cl) with trifluoroacetic acid as previously reported.[42] The electronic and ^1H NMR spectra of the products were identical with those previously reported. N-CD=C(p-C_6H_4Cl)$_2$TPPD was prepared similarly by using trifluoroacetic acid-*d*. The deuteration of the vinyl position was verified by ^1H NMR spectroscopy, which showed that the characteristic resonance at −1.8 ppm had less than 5% of the intensity expected for the ^1H analogue relative to the p-chlorophenyl protons). 2,2-Bis(p-chlorophenyl-d_4)-1,1,1-trichloroethane (DDT) used in the synthesis of N-

(30) Unger, S. W.; Jue, T.; La Mar, G. N. *J. Magn. Reson.*, in press.
(31) Swift, T. J. In "NMR of Paramagnetic Molecules"; La Mar, G. N., Horrocks, W. D., Jr., Holm, R. H., Eds.; Academic Press: New York, 1973; p 53.
(32) Wicholas, M.; Mustacich, R.; Johnson, B.; Smedley, T.; May, J. *J. Am. Chem. Soc.* **1975**, *97*, 2113.
(33) Satterlee, J. D.; La Mar, G. N. *J. Am. Chem. Soc.* **1976**, *98*, 2804.
(34) Mantsch, H. H.; Saito, M.; Smith, I. C. P. *Prog. Nucl. Magn. Reson. Spectrosc.* **1977**, *11*, 211.
(35) La Mar, G. N.; de Ropp, J. S. *J. Am. Chem. Soc.* **1982**, *104*, 5203.
(36) La Mar, G. N.; Budd, D. L.; Goff, H. *Biochem. Biophys. Res. Commun.* **1977**, *77*, 104.
(37) La Mar, G. N.; Jackson, J. T.; Bartsch, R. G. *J. Am. Chem. Soc.* **1981**, *103*, 4405.
(38) Adler, A. D.; Longo, F. R.; Finarelli, J. D.; Goldmacher, J.; Assour, J.; Korsakoff, L. *J. Org. Chem.* **1967**, *32*, 476.
(39) Boersma, A. D.; Goff, H. M. *Inorg. Chem.* **1982**, *21*, 581.
(40) Vaughn, J. D.; Mugharbi, Z.; Wu, E. C. *J. Org. Chem.* **1970**, *35*, 1141.
(41) Lavalle, D. K.; Gebala, A. E. *Inorg. Chem.* **1974**, *13*, 2004.
(42) Lange, M.; Mansuy, D. *Tetrahedron Lett.* **1981**, *22*, 2561.

CH=C(p-C_6D_4Cl)$_2$TPPH was prepared from chloral hydrate and chlorobenzene-d_5 in concentrated sulfuric acid by an established route.[43]

Zinc Complexes. Complexes **9** and **10** were prepared by treating a dichloromethane solution of the appropriate N-alkylporphyrin with a fivefold excess of $ZnCl_2$ in acetonitrile containing 100 μL of 2,2,6,6-tetramethylpiperidine. The solution immediately turned dark green. The solvent was removed and chromatographed on a silica gel column. Dichloromethane was used to elute $TPPH_2$ followed by 10:1 v/v dichloromethane–ethyl acetate to elute the desired zinc complex. The electronic and ^{1}H NMR spectra for **9** were identical with those reported in the literature.[11,44]

Iron(II) Complexes. Complexes **2–7** were prepared by the previously reported method.[9] In a typical reaction dry, dioxygen-free THF (125 mL) was added to anhydrous iron(III) chloride (36.9 mg) and an excess of iron powder. The solution was heated under reflux in a nitrogen atmosphere for 2–3 h. A THF (25 mL) solution of the appropriate N-alkylporphyrin (N-CH_3OEPH, 53.6 mg) was added. The reaction mixture was removed from the heat, and a noncoordinating base (2,2,6,6-tetramethylpiperidine) was added until the solution was slightly basic. After 1 h the solution was filtered through Celite and the solvent was removed. The product was recrystallized from dichloromethane–n-hexane. The crystals were washed with n-hexane to yield 30 mg (48%) of red-green **7**. The electronic spectrum for **7** was similar to that reported for Fe(N-methylprotoporphyrin IX dimethyl ester)Cl.[10] Complexes **2** and **6** give electronic spectra identical with those previously reported. The bromo complex **3** and the iodo complex **4** were obtained by the route described above starting with iron(II) bromide or iron(II) iodide, respectively.

Instrumentation. NMR spectra were obtained on Nicolet NT-360 FT and NMC-500 FT spectrometers operating in the quadrature mode (^{1}H frequencies are 360 and 500 MHz, respectively). Between 200 and 1000 transients were accumulated over a 40-kHz bandwidth with 16K data points for ^{1}H (4–8K for ^{2}H) and a 6-μs 90° pulse. The signal-to-noise ratio was improved by apodization of the free induction decay which introduced a negligible 3–10 Hz of line broadening. Line widths were determined for nonoverlapping peaks by using the Nicolet computer subroutine LF, which fit the peaks to a Lorenzian line. Overlapping peaks were fit by using the NTCCAP routine. The line broadening introduced by apodization was subtracted from the line widths. The peaks were referenced against tetramethylsilane. Electronic spectra were measured with a Hewlett-Packard 8450 A spectrophotometer.

Acknowledgment. We thank the National Institutes of Health (Grant GM26226) for financial support. L.L.-G. was on leave from the Institute of Chemistry, University of Wroclaw, Wroclaw, Poland.

(43) Ginsburg, J. M. *Science (Washington, D.C.)* **1948**, *108*, 339.
(44) Lavellee, D. K. *Bioinorg. Chem.* **1976**, *6*, 219.

Contribution from the Department of Chemistry, Hunter College of CUNY, New York, New York 10021

Effect of N-Substituents and Axial Ligands on Reduction Potentials of N-Substituted Metalloporphyrins

DEBASISH KUILA,[1] ALAN B. KOPELOVE,[2] and DAVID K. LAVALLEE*

Received November 13, 1984

Cyclic voltammetry experiments have been carried out on Fe(II), Mn(II), and Cu(II) complexes of N-substituted porphyrins in order to test the effects of the overall coordination geometry, the N-substituent, and the axial ligand on reduction potentials. In all cases, the complexes exhibited reversible one-electron redox processes attributed to the metal center, specifically involving Fe(III)/Fe(II), Mn(III)/Mn(II), and Cu(II)/Cu(I) oxidation states. The N-substituted porphyrins are the first porphyrins to be reported that exhibit a well-defined Cu(II)/Cu(I) reduction. The half-wave potentials (vs. Ag/AgCl, in CH_3CN with 0.1 M TBAP) for this process are as follows: −0.29 V ([Cu(N-CH_3TPP)]ClO_4); −0.38 V ([Cu(N-CH_3TPP)Cl]); −0.04 V ([Cu(N-CH_3TPP)PPh_3]$^+$); −0.25 V ([Cu(N-C_2H_5TPP)]ClO_4); −0.38 V ([Cu(N-C_2H_5TPP)Cl]); −0.32 V ([Cu(N-PhTPP)]ClO_4); −0.42 V ([Cu(N-PhTPP)Cl]), demonstrating that the axial ligand exhibits a pronounced effect. For each series of complexes, the difference in potentials of the metal-centered process is similar for the N-substituents $-CH_3$, $-CH_2CH_3$, and phenyl (≤0.04 V). The exception to this small effect is the case of chloro(N-p-nitrobenzyl-5,10,15,20-tetraphenylporphinato)manganese(II), which exhibits a Mn(III)/Mn(II) half-wave potential 0.09 V more positive than the corresponding N-methyl or N-ethyl complexes.

Introduction

The N-substituted metalloporphyrins differ markedly from non-N-substituted metalloporphyrins in a number of important respects. While the structural[3] and many of the spectroscopic features (UV–visible absorption and fluorescence,[4] NMR,[4,5] and IR[6] spectra) of these complexes have received considerable attention, there have been few reports of their electrochemical properties.[7] An aspect that we introduce herein is the effect of the N-substituent on reduction potentials. Several other features are also discussed, including identification of a Cu(II)/Cu(I) reduction and measurement of potentials for copper complexes of N-substituted porphyrins with different axial ligands. While it has been shown that reduced states of metal atoms are stabilized in N-substituted metalloporphyrins relative to non-N-substituted analogues, no new oxidation states have been reported. Although many studies have involved the effects of axial ligation on potentials of non-N-substituted metalloporphyrins,[8] there have been no comparable studies for N-substituted metalloporphyrins.

We have previously demonstrated that the stability of N-substituted metalloporphyrins with respect to loss of the N-substituent via nucleophilic attack is highly dependent on the nature of the N-substituent. It appears that the rate of dissociation of the

(1) Current address: Los Alamos Scientific Laboratory, Los Alamos, NM 87545.
(2) M.S. Thesis, Colorado State University, 1981.
(3) Kuila, D.; Lavallee, D. K.; Sauer, C. K.; Anderson, O. P. *J. Am. Chem. Soc.* **1984**, *106*, 448–450 and references therein.
(4) (a) Lavallee, D. K.; McDonough, T. J.; Cioffi, L. *Appl. Spectrosc.* **1982**, *36*, 430–435. (b) Lavallee, D. K.; Bain-Ackerman, M. J. *Bioinorg. Chem.* **1978**, *9*, 311–321. (c) Lavallee, D. K. *Bioinorg. Chem.* **1976**, *6*, 219–227. (d) A wide variety of spectra have also been reported in the papers of Callot: Callot, H. J.; Metz, F. *J. Chem. Soc., Chem. Commun.* **1982**, *947*.
(5) (a) Jackson, A. H. In "The Porphyrins"; Dolphin, D., Ed.; Academic Press: New York, 1978; Vol. 1, pp 341–364. (b) Ortiz de Montellano, P. R.; Kunze, K. L. *J. Am. Chem. Soc.* **1981**, *103*, 6534–6536. (c) Ortiz de Montellano, P. R.; Beilan, H. S.; Matthew, J. M. *J. Med. Chem.* **1982**, *25*, 1174–1179 and references therein. (d) Balch, A. L.; Chan, Y.-W.; Johnson, R.; LaMar, G. N.; Renner, M. *Inorg. Chem. Acta Bioinorg. Chem.* **1983**, *79*, 175.
(6) Lavallee, D. K. *Inorg. Chem.* **1978**, *17*, 231–236.
(7) (a) Lavallee, D. K.; Bain, M. J. *Inorg. Chem.* **1976**, *15*, 2090–2093. (b) Anderson, O. P.; Kopelove, A. B.; Lavallee, D. K. *Inorg. Chem.* **1980**, *19*, 2101–2107. (c) Lavallee, D. K. *J. Inorg. Biochem.* **1982**, *16*, 135–143. (d) Lancon, D.; Cocolios, P.; Guilard, R.; Kadish, K. M. *J. Am. Chem. Soc.* **1984**, *106*, 4472–4478.
(8) (a) Bottomley, L. A.; Kadish, K. M. *Inorg. Chem.* **1981**, *20*, 1348–1357 and reference therein. (b) Kadish, K. M. In "Iron Porphyrins", Part 2; Lever, A. B. P., Gray, H. B., Eds.; Addison-Wesley: Reading, MA, 1983; pp 161–251 and references therein.

0020-1669/85/1324-1443$01.50/0